

Weak Convergence Detection-based Dynamic Reference Point Specification in SMS-EMOA

Weiduo Liao, Ke Shang, Lie Meng Pang, Hisao Ishibuchi

Shenzhen Key Laboratory of Computational Intelligence,

University Key Laboratory of Evolving Intelligent Systems of Guangdong Province,

Department of Computer Science and Engineering,

Southern University of Science and Technology (SUSTech), Shenzhen, China

Email: 11849249@mail.sustech.edu.cn; kshang@foxmail.com; panglm@sustech.edu.cn; hisao@sustech.edu.cn

Abstract—In the evolutionary multi-objective optimization (EMO) field, the hypervolume (HV) indicator is one of the most popular performance indicators. It is not only used for performance evaluation of EMO algorithms (EMOAs) but also adopted in EMOAs for selection (e.g., SMS-EMOA). The specification of a reference point for HV calculation has a large effect on the performance of SMS-EMOA. Thus, the reference point specification should be carefully treated in SMS-EMOA. In this paper, the importance of the dynamic reference point specification in SMS-EMOA is explained first. Then a new dynamic reference point specification mechanism, which is based on weak convergence detection is introduced for SMS-EMOA. Experimental comparisons are conducted for different specification methods in SMS-EMOA: a linearly decreasing mechanism and two static mechanisms. Our results demonstrate the effectiveness of the proposed dynamic reference point specification mechanism.

Keywords—Reference point specification; SMS-EMOA; hypervolume; evolutionary multi-objective optimization; dynamic mechanism; convergence detection

I. INTRODUCTION

In the field of Evolutionary Multi-objective Optimization (EMO) Algorithms, one active research issue is the development of performance indicators. Over the years, various indicators have been proposed. These indicators include hypervolume (HV) [1], R2 [2], ϵ_+ indicator [3], IGD [4], etc. They are designed for different purposes. Each of them has its own advantages and disadvantages. Different from IGD, HV does not need the pre-knowledge of the shape of the Pareto front (PF). HV is also the only Pareto-compliant indicator up to now [5]. However, due to the heavy computation load of HV computation [6], the HV-based algorithms are inefficient when dealing with Many-Objective Optimization Problems (MaOPs) which have more than three objectives.

SMS-EMOA [7] is a classical HV-based algorithm. The HV contribution is used to determine which solution to be discarded in the population. To reduce the heavy computation

load of HV computation, many new methods have been proposed to estimate HV. For example, HypE uses a Monte Carlo simulation technique to estimate HV [8]; the R2 indicator estimates HV using a standard weighted Tchebycheff function [2]; an improved new R2 indicator is proposed by Shang et al. [9] to approximate HV. A simple and fast version of SMS-EMOA, called FV-MOEA [10], has been proposed to further increase the efficiency. FV-MOEA utilizes the fact that the HV contribution of a solution is only determined by partial solutions rather than the whole solution set [10]. Recently, an improved SMS-EMOA with adaptive resource allocation has been proposed to reduce the number of HV calculations [11].

The specification of a reference point is an important issue in HV computation. However, its importance has not been discussed in many studies. Recently, it has been reported that the position of the reference point strongly influences the optimal distribution of solutions for HV maximization in the case of on inverted-triangular Pareto fronts [12]–[14]. A reference point specification method has been proposed in [12] for fair HV computation. A dynamic reference point specification mechanism has been proposed in [15]. Another proposed strategy is to use two reference points in HV-based EMOAs [16].

In this paper, we analyze the reference point specification during the execution of HV-based EMOAs. At the early stage of multi-objective evolution, the reference point should be set far away from the estimated nadir point to enhance the diversity of solutions. In the final stage of multi-objective evolution, the reference point should be specified properly to obtain uniformly distributed solutions over the entire Pareto front.

Based on our analysis, we propose a new dynamic reference point specification mechanism based on weak convergence detection in SMS-EMOA. In our weak convergence detection mechanism, we use the logarithm nadir point as a convergence indicator and use the Simple Least Squares [17] to detect the convergence. We report comparison results of the proposed approach with the existing linearly decreasing method and the simple reference point specification method in the experiment section. On some test problems (e.g., Distance Minimization Problems [18]), our weak convergence detection mechanism outperforms the linearly decreasing mechanism.

This work was supported by National Natural Science Foundation of China (Grant No. 61876075), the Program for Guangdong Introducing Innovative and Entrepreneurial Teams (Grant No. 2017ZT07X386), Shenzhen Peacock Plan (Grant No. KQTD2016112514355531), the Science and Technology Innovation Committee Foundation of Shenzhen (Grant No. ZDSYS201703031748284), and the Program for University Key Laboratory of Guangdong Province (Grant No. 2017KSYS008). Corresponding Author: Hisao Ishibuchi (hisao@sustech.edu.cn)

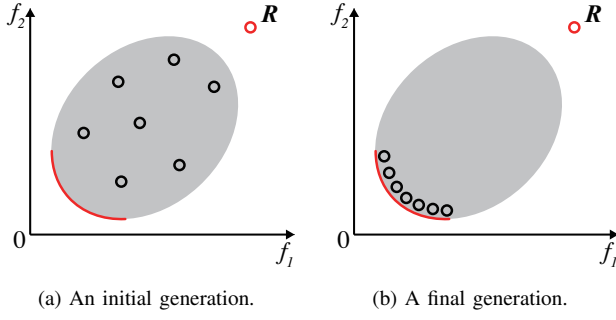


Fig. 1: A reference point R is suitable for the initial population in (a) but too far away from the final population in (b). The gray region shows the feasible region and the red arc is the corresponding Pareto front.

The remainder of this paper is organized as follows. Section II explains the original reference point specification in SMS-EMOA and the one proposed in [12]. Then, we examine the reference point specification in two stages of multi-objective evolution by SMS-EMOA, which clearly demonstrates the necessity of using the dynamic reference point specification mechanism. In Section III, after explaining the existing linearly decreasing method of the reference point, we propose a dynamic reference point specification method. Experimental results by SMS-EMOA with different reference point specification mechanisms on ten-objective triangular and inverted-triangular problems are reported in Section IV. Finally, Section V concludes this paper.

II. REFERENCE POINT SPECIFICATION IN SMS-EMOA

When HV is used in SMS-EMOA, one important issue is how to specify a reference point. Before calculating the HV value, the reference point needs to be specified. However, we cannot specify the fixed reference point using the initial population. A reference point suitable for the initial population is likely to be too far away for the final population as explained in Fig. 1.

In Fig. 2, we show some examples of obtained solution sets by SMS-EMOA. When a fixed reference point is far away from the Pareto front, all solutions are on the sides of the Pareto front when SMS-EMOA is applied to the three-objective inverted DTLZ1 problem [19] in Fig. 2 (a). By appropriately specifying the reference point at each generation (e.g., by Eq. (1) shown later in this section), we can obtain a well-distributed solution set as in Fig. 2 (b). When the Pareto front is triangular, the specification of the reference point does not have a large effect on the finally obtained solution set as shown in Fig. 2 (c) and (d) for the three-objective DTLZ1 problem. For further discussions on the effect of the reference point specification on the distribution of solutions for HV maximization, see [13]–[15].

A. Original Reference Point Specification

In the original paper of SMS-EMOA [7], the reference point is specified as the estimated nadir point increased by 1.0 (in the two-objective case, a sufficiently large reference point is chosen). However in the current implementation of

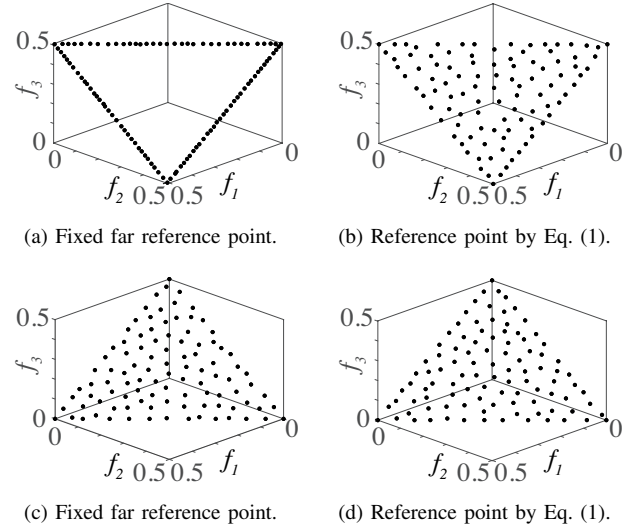


Fig. 2: Obtained solution sets by SMS-EMOA with the population size 100 after 20,000 solution evaluations.

SMS-EMOA in PlatEMO [20], the reference point is specified as:

$$R = r \cdot N, \quad (1)$$

where $R \in \mathbb{R}^m$ is the reference point in each generation, and $N \in \mathbb{R}^m$ is the estimated nadir point of the last front from the current population. r is specified as 1.1 in PlatEMO. In the source code of PlatEMO, the values of r in HV-based algorithms are specified as follows: 1.1 (SMS-EMOA [7]) and 1.2 (HypE [8]). In SMS-EMOA, the HV contribution is used to evaluate each solution. We specify the reference point for HV calculation by Eq. (1) in this paper.

However, fixing the r value to 1.1 is not recommended, especially for problems with inverted-triangular Pareto fronts [12]. The research on specifying the value of r is limited. This is because the location of the reference point does not have a large effect on the calculation of HV contribution when HV-based algorithms are applied to test problems with triangular Pareto fronts.

B. Reference Point Specification Proposed in [12]

In [12]–[14], an appropriate value of r was suggested from a viewpoint of fair HV-based performance comparison of EMO algorithms. The suggested r is:

$$r = 1 + \frac{1}{H}, \quad (2)$$

where H is a parameter used in MOEA/D [21] for generating uniformly distributed weight vectors [15]. Given the population size μ and the number of objectives m , the value of H can be calculated as follows:

$$C_{m-1}^{H+m-1} \leq \mu < C_{m-1}^{H+m}. \quad (3)$$

In Fig. 3 (a), $r = 13/12$ ($H = 12$) is the suggested setting in [12] for inverted-DTLZ1 with $\mu = 91$ and $m = 3$. Well-distributed solutions are obtained in Fig. 3 (a). In Fig. 3 (b)-(d),

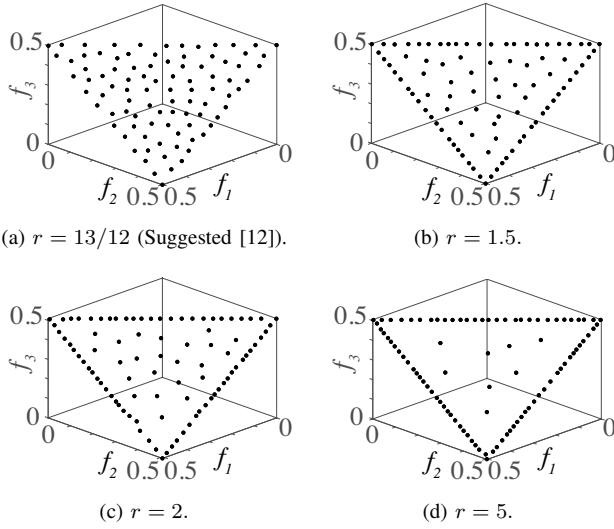


Fig. 3: Obtained solution sets for the three-objective inverted DTLZ1 problem by SMS-EMOA with different specifications of the reference point r . The population size is 91 ($H = 12$) and the stopping condition is 20,000 solution evaluations.

the increase of r (i.e., the increase of the distance between the estimated nadir point and the reference point) increases the number of solutions on the sides of the inverted triangular Pareto front.

Very roughly speaking, multi-objective evolution by EMOAs can be divided into the following two stages:

1) *Early Stage*: In this stage, all solutions are far away from the Pareto front. The main task is to converge the solutions to the Pareto front. We also call this stage the convergence stage.

2) *Final Stage*: In this stage, all solutions are on or near the Pareto front. So the main task is to distribute the solutions more evenly on the Pareto front. We also call this stage the diversification stage.

C. Specify the Value of r for Better Searching Behavior

Fig. 4 shows obtained solution sets by SMS-EMOA with different specifications of r on the ten-objective DTLZ2 problem. It can be observed that, when r is set to 2, the solutions for the first six dimensions in Fig. 4 (b) are all 0. This phenomenon shows that the breadth-diversity [22] in Fig. 4 (b) is worse than that in Fig. 4 (a), although $r = 2$ is the suggested value for r in this experimental setting.

If we set $r = 1 + 1/H$ at the early stage of the algorithm, the exploration of solutions will be poor. So, a larger value of r than $1 + 1/H$ is suggested in the early stage [15].

D. Specify the Value of r for Uniform Distribution

When the algorithm reaches the final stage of the algorithm, all solutions are near the Pareto front. To get a uniform solution distribution, r should be specified as $1 + 1/H$, as in Eq. (2). For problems with inverted-triangular Pareto fronts, the distribution of obtained solutions strongly depends on the value of r (as shown in Fig. 3).

Strong sensitivity of the distribution of obtained solutions on the value of r is also observed on some other problems

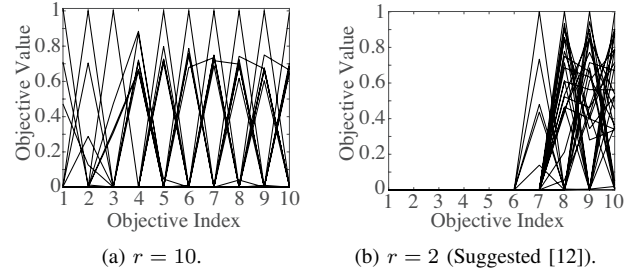


Fig. 4: Obtained solution sets for the ten-objective DTLZ2 problem by SMS-EMOA with different specifications of the reference point r . The population size is 30 ($H = 1$) and the stopping condition is 10,000 solution evaluations.

(e.g., Distance Minimization Problems [18]). This observation suggests the potential usefulness of the dynamic reference point specification [15].

III. DYNAMIC REFERENCE POINT SPECIFICATION MECHANISM

Since a different stage of multi-objective evolution has a different purpose, the value of r should be treated differently in each stage [15]. Not only the estimated nadir point but also the value of r needs to be adapted in each iteration of the algorithm. This is called dynamic reference point specification. Based on Eq. (1), we define the dynamic reference point specification as:

$$\mathbf{R} = r(t) \cdot \mathbf{N}, \quad t = 0, 1, \dots, T, \quad (4)$$

where T is the total number of generations, and $r(t)$ is a function of the current generation t . The value of r is specified by $r(t)$.

A. Linearly Decreasing Mechanism Proposed in [15]

Based on the description above, r is suggested to be specified dynamically at different stages of the algorithm (at the early stage, a larger r is specified; at the final stage, $r = 1 + 1/H$ is specified).

In [15], a linearly decreasing mechanism has been proposed:

$$r(t) = r_{Initial} \frac{(T-t)}{T} + (1+1/H) \frac{t}{T}, \quad t = 0, 1, \dots, T, \quad (5)$$

where T is the total number of generations, and $r_{Initial}$ is the initial value of r , which is larger than $1 + 1/H$. It is a simple and practical mechanism. In Eq. (5), the value of r starts from $r_{Initial}$, then gradually decreases to the suggested value in a linearly decreasing manner.

In the next section, another dynamic mechanism based on weak convergence detection criterion is proposed. We show that it outperforms the simple linearly decreasing mechanism on some test problems.

B. A New Dynamic Reference Point Specification Mechanism

In this section, we introduce a new mechanism that uses a weak convergence detection criterion to decide the timing of changing the value of r from $r_{Initial}$ to $1 + 1/H$.

As we have explained before, a larger r is suggested at the early stage of the algorithm. But for good uniformity at the

final stage, it is needed to set r to its suggested value $1 + 1/H$. For this purpose, it is necessary to detect whether the algorithm is converged. If solutions are all close to the Pareto front, we change the value of r to $1 + 1/H$; otherwise, we set the value of r to $r_{Initial}$. The mechanism is shown below:

$$r(t) = \begin{cases} r_{Initial}, & t < t_{Converged}, \\ 1 + 1/H, & t \geq t_{Converged}, \end{cases} \quad t = 0, 1, \dots, T. \quad (6)$$

$r(t)$ equals to $r_{Initial}$ before reaching the converged generation $t_{Converged}$, and changes to $1 + 1/H$ after $t_{Converged}$. $t_{Converged}$ is determined by a weak convergence detection criterion.

Various indicators including convergence detection indicators which are used to detect the stagnation of the algorithm have been proposed in the literature [23]–[29]. They focus on accurately detecting the convergence, which is not the purpose in our approach. After the algorithm has converged, we still need some generations in order to get uniformly distributed solutions. We summarize the required conditions for our weak convergence detection as follows:

1) *Moderately accurate*: It is not necessary to have a very accurate convergence detection. The convergence can be reported if all of the current solutions are close to the Pareto front. In other words, the estimated ideal and nadir points based on the current solutions are close to the true ideal and nadir points.

2) *Computationally efficient*: We should not spend too much time on convergence detection. The state-of-the-art HV-based algorithms (e.g., SMS-EMOA and HypE) are time-consuming when the dimension of the objective space is very high.

HV is not a good choice as our weak convergence detection indicator. The reason is that during the execution of the algorithm, the reference point is calculated by Eq. (1), which means that they are different over generations. So, we cannot simply compare calculated HV values at different generations.

We should consider other indicators that satisfy the above-mentioned two conditions. During the execution of the algorithm, the HV of the current population increases while the estimated nadir point from the current population is gradually approaching the Pareto front. The estimated nadir point can be a good choice for our purpose. More specifically, for a minimization problem, we consider the following indicator I :

$$\begin{aligned} \mathbf{N}_t &= [f_{t1}, f_{t2}, \dots, f_{tm}]^T \in \mathbb{R}^m, \\ I_0 &= \frac{1}{m} \sum_{i=1}^m \ln f_{0i}, \\ I_t &= \min(I_{t-1}, \frac{1}{m} \sum_{i=1}^m \ln f_{ti}), \quad t = 1, 2, \dots, T, \end{aligned} \quad (7)$$

where T is the total number of generations, \mathbf{N}_t is the estimated nadir point at the t^{th} generation with m elements: $f_{t1}, f_{t2}, \dots, f_{tm}$. I_0 is the average logarithmic element value of the nadir point calculated from the initial population. I_t is the minimum value of I before the t^{th} generation (including

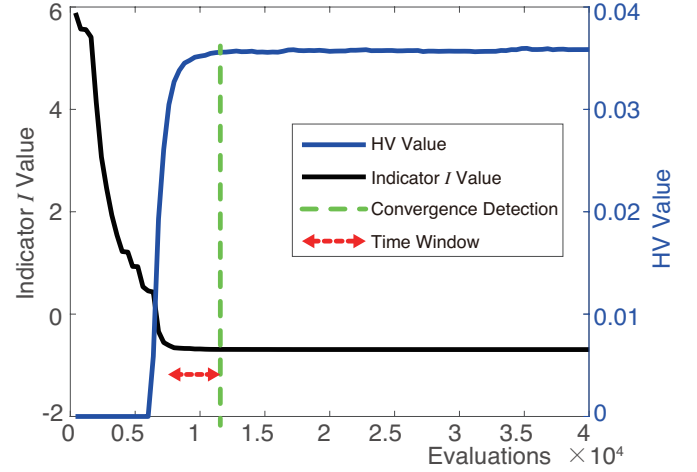


Fig. 5: Illustration of the convergence detection for a run of SMS-EMOA on the three-objective inverted-DTLZ1 problem. The fixed reference point $\mathbf{R} = (0.55, 0.55, 0.55)$ is used for HV calculation in this figure.

the t^{th} generation). Fig. 5 shows the HV values and the indicator I values over the execution of SMS-EMOA on the three-objective inverted-DTLZ1 problem. The fixed nadir point based on the true nadir point is used for HV calculation in this figure for illustration purposes: $\mathbf{R} = (0.55, 0.55, 0.55)$. When the current solutions are close to the Pareto front (i.e., the HV value reaches the stagnation), the convergence should be reported. Meanwhile, the estimated nadir point of the current solutions is close to the true nadir point (i.e., the indicator I value also reaches the stagnation).

After choosing the indicator, the next step is to detect the stagnation of the indicator. We use a basic linear regression method called Simple Least Squares [17] with a simple least squares convergence detection strategy introduced in [24]. If the absolute value of the slope of the linear regression is below a threshold, the convergence is reported. Briefly speaking, considering a simple linear regression model $I(t) = a + bt$, the intercept a and slope b of the t^{th} generation can be calculated with the following matrix-based formula:

$$\begin{bmatrix} a \\ b \end{bmatrix} = \begin{bmatrix} \sum t_i^2 & \sum t_i \\ \sum t_i & w_l \end{bmatrix}^{-1} * \begin{bmatrix} \sum t_i I_{t_i} \\ \sum I_{t_i} \end{bmatrix}, \quad (8)$$

where w_l is the length of the chosen time window (in the example of Fig. 5, the chosen time window is represented with the red dotted line), and t_i is the time index in the chosen time window, $t_i \in (t', t]$, $t - t' = w_l$. The absolute value of slope b is shown in Fig. 6 (Note that in the first w_l evaluations is 0, and we should not consider the first w_l evaluations).

Using Eq. (8), we report the convergence of the algorithm if the following condition holds:

$$|b| < thres. \quad (9)$$

We choose $thres$ value as 10^{-5} after some computational experiments with the window size w_l of 4,000. The choice of the threshold value $thres$ does not have a strong effect on the performance of the proposed HV-based algorithm since the

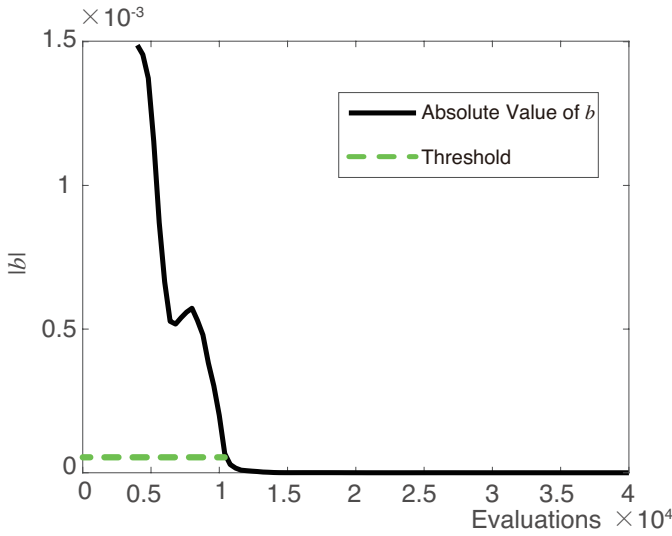


Fig. 6: Values of $|b|$ for the three-objective inverted-DTLZ1 (the window size w_l is 4,000 and the population size μ is 100). The green dotted line shows the threshold 10^{-5} .

accuracy of the convergence detection is not very important. The whole process of the weak convergence detection is described in Algorithm 1. If Algorithm 1 returns True, we report the convergence. The value of the converged generation $t_{Converged}$ equals to t (i.e., the current evaluation number) when the convergence is detected.

Algorithm 1: Weak Convergence Detection

Input:

w_l , // Window size.
 S_t , // Solution set when evaluation number is t .
 $I = \{I_0, I_1, \dots, I_{t-1}\}$, // Stored indicator values.
 $thres$, // The chosen threshold for slope.

Output: Return True if converged, otherwise return False.

Calculate nadir point N_t of S_t ;
 Calculate indicator I_t ; // By Eq. (7).
 $I \leftarrow I \cup \{I_t\}$;
if $t \geq w_l$ **then**
 Calculate b ; // By Eq. (8).
 if $|b| < thres$ **then**
 Return True; // Converged.
 end if
end if
 Return False; // Not converged.

IV. COMPUTATIONAL EXPERIMENTS

A. Experimental Settings

In this section, the two different dynamic reference point specification mechanisms (i.e., the linearly decreasing mechanism and the weak convergence detection mechanism) are tested by combining each of them into SMS-EMOA [7].

The DTLZ test suite [30], WFG test suite [31], their minus-versions [32], and Multi-Point Distance Minimization Problems (MPDMP) [18] are used in our computational experiments. The number of objectives (m) is specified as 10 in all test problems. The number of decision variables (D) is specified for each test problem as follows:

- 14 (DTLZ1 and minus-DTLZ1),
- 2 (MPDMP),
- 19 (other problems).

All codes in this section are implemented in PlatEMO framework [20] with the following settings:

- Population size: 30 ($H = 1$),
- Stopping condition: 100,000 solution evaluations,
- Crossover: Simulated binary crossover,
- Crossover probability: 1.0,
- Mutation: Polynomial mutation,
- Mutation probability: $1/D$,
- Distribution index of Crossover and Mutation: 20,
- Number of runs: 20 runs.

B. Computational Results

In our experiments, four versions of SMS-EMOA with different reference point specification mechanisms are considered. These algorithms are named as SMS-EMOA-10, SMS-EMOA-Opt, SMS-EMOA-LD, and SMS-EMOA-CD. For SMS-EMOA-10, the value of r is set to 10. The value of r for SMS-EMOA-Opt is set to $r = 1 + 1/H$ (Here $H = 1$). SMS-EMOA with the linearly decreasing mechanism and with the weak convergence detection mechanism are referred to as SMS-EMOA-LD and SMS-EMOA-CD, respectively. In both of the two specification methods, the initial value of r ($r_{Initial}$) is 10, and its final value is $1 + 1/H$ (Here $H = 1$). The average HV value is calculated over 20 runs of each algorithm on each test problem under the stopping condition of 100,000 solution evaluations. The reference point is specified as 2 times the true nadir point for HV performance comparison. Table I and Table II show HV-based comparison results. The best result in each row is highlighted in bold, and the worst result is shaded. The Wilcoxon rank sum test is used to show the statistical significance for SMS-EMOA-10, SMS-EMOA-Opt, SMS-EMOA-LD in comparison with the proposed SMS-EMOA-CD. The three symbols “+”, “−”, “ \approx ” mean significantly better, significantly worse and no significant difference.

Table I shows that SMS-EMOA-Opt performs the worst (significantly worse than SMS-EMOA-CD for 9 out of the 13 test problems) among the compared algorithms. This observation suggests that the use of $r = 1 + 1/H$ throughout the execution of SMS-EMOA is not a good idea. We cannot tell the differences between SMS-EMOA-10 and SMS-EMOA-CD. The Wilcoxon rank sum tests show that almost all the results are “ \approx ”. This is because that the location of the reference point has no influence on the optimal distribution of solutions for HV maximization when Pareto fronts are triangular and the reference point is not too close to the Pareto front. For two test problems (WFG8 and WFG9), better results

Table I: Mean HV and standard deviation over 20 independent runs for DTLZ and WFG test problems.

Problem	M	D	SMS-EMOA-10	SMS-EMOA-Opt	SMS-EMOA-LD	SMS-EMOA-CD
DTLZ1	10	14	6.8448e-1 (4.61e-1) \approx	2.0261e-1 (2.23e-1) $-$	8.8369e-1 (2.00e-1) \approx	6.9062e-1 (3.95e-1)
DTLZ2	10	19	1.0234e+3 (4.72e-1) \approx	9.9315e+2 (3.94e+1) $-$	1.0234e+3 (7.28e-1) \approx	1.0184e+3 (1.85e+1)
DTLZ3	10	19	0.0000e+0 (0.00e+0) \approx	1.9068e+1 (8.53e+1) \approx	0.0000e+0 (0.00e+0) \approx	0.0000e+0 (0.00e+0)
DTLZ4	10	19	8.0029e+2 (2.21e+2) \approx	5.2691e+2 (1.79e+2) $-$	6.6262e+2 (2.17e+2) \approx	7.2840e+2 (2.26e+2)
WFG1	10	19	2.2025e+12 (2.55e+11) \approx	2.2597e+12 (2.64e+11) \approx	2.2005e+12 (1.81e+11) \approx	2.2601e+12 (3.42e+11)
WFG2	10	19	3.3604e+12 (2.92e+10) \approx	3.3493e+12 (2.39e+10) $+$	3.3487e+12 (7.64e+10) \approx	3.3420e+12 (8.46e+10)
WFG3	10	19	4.7217e-3 (1.04e-2) $-$	2.5310e-2 (3.07e-2) \approx	1.7230e-2 (2.35e-2) \approx	2.3443e-2 (2.84e-2)
WFG4	10	19	3.7667e+12 (1.77e+10) \approx	3.5602e+12 (9.48e+10) $-$	3.7585e+12 (3.74e+10) \approx	3.7737e+12 (1.63e+10)
WFG5	10	19	3.6535e+12 (7.68e+9) \approx	3.5027e+12 (1.16e+11) $-$	3.6555e+12 (8.64e+9) \approx	3.6523e+12 (1.93e+10)
WFG6	10	19	3.6082e+12 (7.78e+10) \approx	3.5432e+12 (6.24e+10) $-$	3.5829e+12 (5.75e+10) \approx	3.6099e+12 (4.49e+10)
WFG7	10	19	3.7967e+12 (7.58e+9) \approx	3.7326e+12 (5.73e+10) $-$	3.7959e+12 (1.35e+10) \approx	3.7922e+12 (1.27e+10)
WFG8	10	19	3.7512e+12 (1.51e+10) \approx	3.7087e+12 (3.64e+10) $-$	3.7613e+12 (1.13e+10) $+$	3.7524e+12 (1.23e+10)
WFG9	10	19	3.5727e+12 (1.85e+11) \approx	3.3072e+12 (2.80e+11) $-$	3.6302e+12 (1.57e+11) $+$	3.5146e+12 (2.31e+11)
$+/-/\approx$			0/1/12	1/9/3	2/0/11	

Table II: Mean HV and standard deviation over 20 independent runs for minus-DTLZ, minus-WFG and MPDMP.

Problem	M	D	SMS-EMOA-10	SMS-EMOA-Opt	SMS-EMOA-LD	SMS-EMOA-CD
minus-DTLZ1	10	14	4.3889e+28 (5.56e+26) \approx	4.4237e+28 (5.99e+26) \approx	4.4120e+28 (4.79e+26) \approx	4.3872e+28 (7.72e+26)
minus-DTLZ2	10	19	1.2299e+7 (1.38e+5) $-$	1.4737e+7 (1.55e+5) $-$	1.4891e+7 (1.11e+5) \approx	1.4844e+7 (1.45e+5)
minus-DTLZ3	10	19	1.1227e+35 (3.16e+33) $-$	1.3385e+35 (3.41e+33) \approx	1.3702e+35 (3.42e+33) \approx	1.3582e+35 (3.78e+33)
minus-DTLZ4	10	19	1.1638e+7 (2.11e+5) $-$	1.4899e+7 (1.20e+5) $+$	1.4895e+7 (1.27e+5) $+$	1.3585e+7 (1.57e+6)
minus-WFG1	10	19	4.4808e+10 (5.25e+8) \approx	4.4894e+10 (4.81e+8) \approx	4.4890e+10 (4.35e+8) \approx	4.4705e+10 (5.60e+8)
minus-WFG2	10	19	6.6225e+10 (1.05e+8) $-$	6.7628e+10 (7.51e+8) \approx	6.7870e+10 (3.31e+7) $-$	6.7907e+10 (1.60e+7)
minus-WFG3	10	19	6.3620e+10 (5.49e+8) \approx	6.4321e+10 (2.29e+8) $+$	6.3642e+10 (4.93e+8) \approx	6.3799e+10 (5.87e+8)
minus-WFG4	10	19	1.6478e+11 (3.22e+9) $-$	1.9896e+11 (2.20e+9) \approx	1.9752e+11 (2.39e+9) \approx	1.9260e+11 (1.34e+10)
minus-WFG5	10	19	1.6534e+11 (2.09e+9) $-$	1.9817e+11 (1.82e+9) \approx	1.9897e+11 (1.93e+9) \approx	1.9819e+11 (1.40e+9)
minus-WFG6	10	19	1.6532e+11 (2.11e+9) $-$	1.9865e+11 (1.83e+9) \approx	1.9989e+11 (2.03e+9) \approx	1.9960e+11 (1.94e+9)
minus-WFG7	10	19	1.6534e+11 (2.88e+9) $-$	1.9870e+11 (1.30e+9) $-$	1.9978e+11 (2.21e+9) \approx	1.9937e+11 (2.97e+9)
minus-WFG8	10	19	1.6808e+11 (1.46e+9) $-$	1.9932e+11 (1.56e+9) $-$	2.0220e+11 (1.71e+9) $+$	2.0065e+11 (1.77e+9)
minus-WFG9	10	19	1.6415e+11 (3.16e+9) $-$	1.9777e+11 (2.21e+9) \approx	1.9557e+11 (2.17e+9) $-$	1.9852e+11 (1.86e+9)
MPDMP	10	2	1.4848e+5 (2.50e+2) $-$	1.5051e+5 (3.10e+2) $-$	1.5017e+5 (1.98e+2) $-$	1.5097e+5 (1.64e+2)
$+/-/\approx$			0/11/3	2/4/8	2/3/9	

are obtained from SMS-EMOA-LD than SMS-EMOA-CD. For all the other test problems, these two algorithms have no statistically significant differences. These observations suggest that SMS-EMOA-LD is slightly better than SMS-EMOA-CD on test problems with triangular Pareto fronts.

Table II shows HV-based performance comparison results on test problems with inverted-triangular Pareto front (i.e., minus-DTLZ1-4, minus-WFG1-9, and MPDMP). In Table II, SMS-EMOA-10 performs the worst on most test problems (12 out of the 14 test problems). The Wilcoxon rank sum tests show that SMS-EMOA-10 is significantly outperformed by SMS-EMOA-CD on 11 out of the 14 test problems. This result can be explained by the setting of r . Since the value of r is set to 10 in SMS-EMOA-10, many solutions are on the boundary of the triangular Pareto fronts. In Table II, it seems that

the other three algorithms (SMS-EMOA-Opt, SMS-EMOA-LD and SMS-EMOA-CD) have almost the same performance on the test problems with inverted-triangular Pareto front. The results of MPDMP shows that SMS-EMOA-CD is the best among the four algorithms.

Fig. 7 shows the average HV values for the four algorithms on the ten-objective MPDMP problem. In Fig. 7, the HV value by SMS-EMOA-LD (the red curve) gradually increases and finally reaches the same level as SMS-EMOA-Opt. This is because the value of r is gradually decreased to $1 + 1/H$. The HV value by SMS-EMOA-CD (the yellow curve) reaches a stable level similar to SMS-EMOA-10. This is because the value of r in these two algorithms is 10 for about 4,500 evaluations. The convergence detection is reported after about 4,500 evaluations in each of the 20 runs of SMS-EMOA-

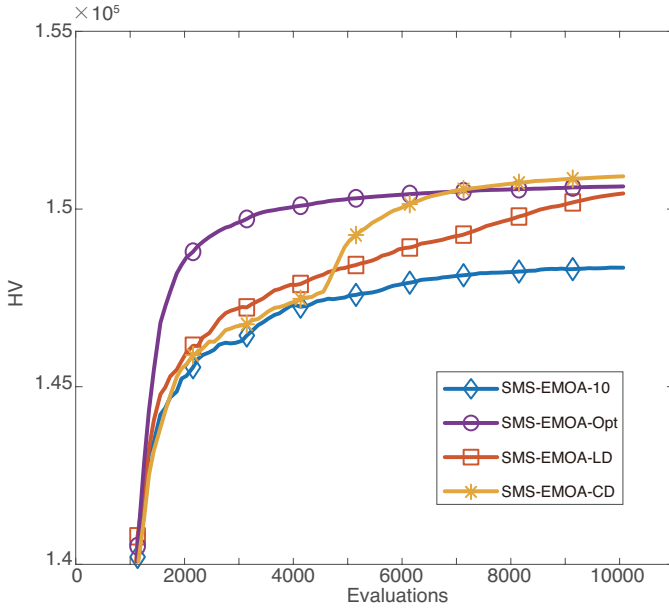


Fig. 7: Average HV values by the four algorithms on the ten-objective Multi-Point Distance Minimization Problem (MPDMP).

CD. Then, the value of r in SMS-EMOA-CD is changed to $1 + 1/H$. After this change, the HV value quickly increases. This quick increase of the HV value is due to the increase of inner solutions (and the decrease of boundary solutions). Finally, the HV value by SMS-EMOA-CD is better than SMS-EMOA-10, SMS-EMOA-Opt and SMS-EMOA-LD after 10,000 solution evaluations.

V. CONCLUSIONS

In this paper, first we explain the importance of an appropriate reference point specification in SMS-EMOA using a simple example. We demonstrate that, without a good reference point specification mechanism, well-distributed solutions are not obtained on inverted triangular Pareto fronts. This is not observed for triangular Pareto fronts. That is, well-distributed solutions are obtained when the reference point is not too close to the triangular Pareto fronts.

Next we summarize the basic idea of the dynamic reference point specification mechanism as follows: the value of r should be specified larger than $1 + 1/H$ at the early stage for better searching behavior and equal to $1/(1 + H)$ at the final stage to get a uniform solution distribution, as in Eqs. (4)-(6).

After that, we propose a new dynamic reference point specification mechanism in this paper. A weak convergence detection mechanism is used in the proposed method. The new dynamic reference point specification mechanism is tested on SMS-EMOA algorithm and compared with other SMS-EMOAs under different settings of r . The results show that SMS-EMOA with $r = 1 + 1/H$ performs the worst on the triangular PF problems, and SMS-EMOA with $r = 10$ performs the worst on the inverted-triangular PF problems. This gives us a hint on the necessary of the dynamic mechanism. We have also compared our proposed mechanism with the

linearly decreasing mechanism. The results show that our new mechanism outperforms the linearly decreasing mechanism on some test problems, specifically on the MPDMP.

In the future, we plan to investigate the behavior of our new mechanism and further improve it. The problems with different PF shapes will be tested and analyzed.

REFERENCES

- [1] E. Zitzler and L. Thiele, "Multiobjective optimization using evolutionary algorithms—A comparative case study," in *Parallel Problem Solving from Nature*, V. Berlin, Germany: Springer-Verlag, 1998, pp. 292–301.
- [2] M. P. Hansen and A. Jaszkiewicz, *Evaluating the Quality of Approximations to the Non-dominated Set*. IMM, Department of Mathematical Modelling, Technical University of Denmark, 1994.
- [3] E. Zitzler, L. Thiele, M. Laumanns, C. M. Fonseca, and V. G. da Fonseca, "Performance assessment of multiobjective optimizers: An analysis and review," *IEEE Transactions on Evolutionary Computation*, vol. 7, no. 2, pp. 117–132, Apr. 2003. [Online]. Available: <http://dx.doi.org/10.1109/TEVC.2003.810758>
- [4] C. A. C. Coello and M. R. Sierra, "A study of the parallelization of a coevolutionary multi-objective evolutionary algorithm," in *Mexican International Conference on Artificial Intelligence*. Springer, 2004, pp. 688–697.
- [5] E. Zitzler, D. Brockhoff, and L. Thiele, "The hypervolume indicator revisited: On the design of pareto-compliant indicators via weighted integration," in *International Conference on Evolutionary Multi-Criterion Optimization*. Springer, 2007, pp. 862–876.
- [6] N. Beume, C. M. Fonseca, M. Lopez-Ibanez, L. Paquete, and J. Vahrenhold, "On the complexity of computing the hypervolume indicator," *IEEE Transactions on Evolutionary Computation*, vol. 13, no. 5, pp. 1075–1082, 2009.
- [7] N. Beume, B. Naujoks, and M. Emmerich, "SMS-EMOA: Multiobjective selection based on dominated hypervolume," *European Journal of Operational Research*, vol. 181, no. 3, pp. 1653–1669, 2007.
- [8] J. Bader and E. Zitzler, "HypE: An algorithm for fast hypervolume-based many-objective optimization," *Evolutionary Computation*, vol. 19, no. 1, pp. 45–76, 2011.
- [9] K. Shang, H. Ishibuchi, M.-L. Zhang, and Y. Liu, "A new R2 indicator for better hypervolume approximation," in *Proceedings of the Genetic and Evolutionary Computation Conference*, ser. GECCO '18. New York, NY, USA: ACM, 2018, pp. 745–752. [Online]. Available: <http://doi.acm.org/10.1145/3205455.3205543>
- [10] S. Jiang, J. Zhang, Y.-S. Ong, A. N. Zhang, and P. S. Tan, "A simple and fast hypervolume indicator-based multiobjective evolutionary algorithm," *IEEE Transactions on Cybernetics*, vol. 45, no. 10, pp. 2202–2213, 2014.
- [11] A. Menchaca-Méndez, E. Montero, and S. Zapotecas-Martínez, "An improved s-metric selection evolutionary multi-objective algorithm with adaptive resource allocation," *IEEE Access*, vol. 6, pp. 63 382–63 401, 2018.
- [12] H. Ishibuchi, R. Imada, S. Yu, and Y. Nojima, "How to specify a reference point in hypervolume calculation for fair performance comparison," *Evolutionary Computation*, vol. 26, no. 3, pp. 1–29, 2018.
- [13] H. Ishibuchi, R. Imada, Y. Setoguchi, and Y. Nojima, "Reference point specification in hypervolume calculation for fair comparison and efficient search," in *Proceedings of the Genetic and Evolutionary Computation Conference*. ACM, 2017, pp. 585–592.
- [14] —, "Hypervolume subset selection for triangular and inverted triangular pareto fronts of three-objective problems," in *Proceedings of the 14th ACM/SIGEVO Conference on Foundations of Genetic Algorithms*. ACM, 2017, pp. 95–110.
- [15] H. Ishibuchi, R. Imada, N. Masuyama, and Y. Nojima, "Dynamic specification of a reference point for hypervolume calculation in SMS-EMOA," in *2018 IEEE Congress on Evolutionary Computation (CEC)*. IEEE, 2018, pp. 1–8.
- [16] —, "Use of two reference points in hypervolume-based evolutionary multiobjective optimization algorithms," in *International Conference on Parallel Problem Solving from Nature*. Springer, 2018, pp. 384–396.
- [17] P. L. Meyer, *Introductory Probability and Statistical Applications*. Addison-Wesley Publishing Company, 1970.

- [18] H. Ishibuchi, K. Doi, and Y. Nojima, "On the effect of normalization in MOEA/D for multi-objective and many-objective optimization," *Complex & Intelligent Systems*, vol. 3, no. 4, pp. 279–294, 2017.
- [19] H. Jain and K. Deb, "An evolutionary many-objective optimization algorithm using reference-point based nondominated sorting approach, part II: handling constraints and extending to an adaptive approach," *IEEE Transactions on Evolutionary Computation*, vol. 18, no. 4, pp. 602–622, 2013.
- [20] Y. Tian, R. Cheng, X. Zhang, and Y. Jin, "PlatEMO: A MATLAB platform for evolutionary multi-objective optimization [educational forum]," *IEEE Computational Intelligence Magazine*, vol. 12, no. 4, pp. 73–87, 2017.
- [21] Q. Zhang and H. Li, "MOEA/D: A multiobjective evolutionary algorithm based on decomposition," *IEEE Transactions on Evolutionary Computation*, vol. 11, no. 6, pp. 712–731, 2007.
- [22] Z. Wang, Y.-S. Ong, J. Sun, A. Gupta, and Q. Zhang, "A generator for multiobjective test problems with difficult-to-approximate pareto front boundaries," *IEEE Transactions on Evolutionary Computation*, 2018.
- [23] H. Trautmann, U. Ligges, J. Mehnen, and M. Preuss, "A convergence criterion for multiobjective evolutionary algorithms based on systematic statistical testing," in *International Conference on Parallel Problem Solving from Nature*. Springer, 2008, pp. 825–836.
- [24] J. L. Guerrero, L. Martí, A. Berlanga, J. García, and J. M. Molina, "Introducing a robust and efficient stopping criterion for MOEAs," in *IEEE Congress on Evolutionary Computation*. IEEE, 2010, pp. 1–8.
- [25] T. Wagner, H. Trautmann, and B. Naujoks, "OCD: Online convergence detection for evolutionary multi-objective algorithms based on statistical testing," in *International Conference on Evolutionary Multi-Criterion Optimization*. Springer, 2009, pp. 198–215.
- [26] H. Trautmann, T. Wagner, B. Naujoks, M. Preuss, and J. Mehnen, "Statistical methods for convergence detection of multi-objective evolutionary algorithms," *Evolutionary Computation*, vol. 17, no. 4, pp. 493–509, 2009.
- [27] K. Deb and S. Jain, "Running performance metrics for evolutionary multi-objective optimization," Tech. Rep., 2002.
- [28] O. Rudenko and M. Schoenauer, "A steady performance stopping criterion for pareto-based evolutionary algorithms," in *6th International Multi-Objective Programming and Goal Programming Conference*, 2004.
- [29] T. Wagner, H. Trautmann, and L. Martí, "A taxonomy of online stopping criteria for multi-objective evolutionary algorithms," in *International Conference on Evolutionary Multi-Criterion Optimization*. Springer, 2011, pp. 16–30.
- [30] K. Deb, L. Thiele, M. Laumanns, and E. Zitzler, "Scalable multi-objective optimization test problems," in *Proceedings of the 2002 Congress on Evolutionary Computation. CEC'02 (Cat. No. 02TH8600)*, vol. 1. IEEE, 2002, pp. 825–830.
- [31] S. Huband, P. Hingston, L. Barone, and L. While, "A review of multiobjective test problems and a scalable test problem toolkit," *IEEE Transactions on Evolutionary Computation*, vol. 10, no. 5, pp. 477–506, 2006.
- [32] H. Ishibuchi, Y. Setoguchi, H. Masuda, and Y. Nojima, "Performance of decomposition-based many-objective algorithms strongly depends on pareto front shapes," *IEEE Transactions on Evolutionary Computation*, vol. 21, no. 2, pp. 169–190, 2016.